Ge/C Nanowires as High-Capacity and Long-Life Anode Materials for Li-Ion Batteries

Jun Liu,[‡] Kepeng Song,[§] Changbao Zhu,[‡] Chia-Chin Chen,[‡] Peter A. van Aken,[§] Joachim Maier,[‡] and Yan Yu[†,‡,*]

[†]CAS Key Laboratory of Materials for Energy Conversion, Department of Materials Science and Engineering, University of Science and Technology of China, Hefei 230026, Anhui, China, [‡]Max Planck Institute for Solid State Research, Heisenbergstr. 1, Stuttgart 70569, Germany, and [§]Max Planck Institute for Intelligent Systems, Heisenbergstr. 3, Stuttgart 70569, Germany

ABSTRACT Germanium-based materials (Ge and GeO_x) have recently demonstrated excellent lithium-ion storage ability and are being considered as the most promising candidates to substitute commercial carbon-based anodes of lithium-ion batteries. Nevertheless, practical implementation of Ge-based materials to lithium-ion batteries is greatly hampered by the poor cyclability that resulted from the huge volume variation during lithiation/delithiation processes. Herein, uniform carbon-encapsulated Ge and GeO_x nanowires were synthesized by a one-step controlled pyrolysis of organic–inorganic hybrid GeO_x/ethylenediamine (GeO_x/EDA) nanowires in H_2/Ar and Ar atmospheres, respectively. The as-obtained Ge/C and GeO_x/C nanowires possess well-defined 0D-in-1D morphology and homogeneous carbon encapsulation, which exhibit excellent Li storage properties including high specific capacities (approximate 1200 and 1000 mA h g^{-1} at 0.2C for Ge/C and GeO_x/C, respectively). The Ge/C nanowires, in particular, demonstrate superior rate capability with excellent capacity retention and stability (producing high stable discharge capacities of about 770 mA h g^{-1} after 500 cycles at 10C), making them promising candidates for future electrodes for high-power Li-ion batteries. The improved electrochemical performance arises from synergistic effects of 0D-in-1D morphology and uniform carbon coating, which could effectively accommodate the huge volume change of Ge/GeO_x during cycling and maintain perfect electrical conductivity throughout the electrode.

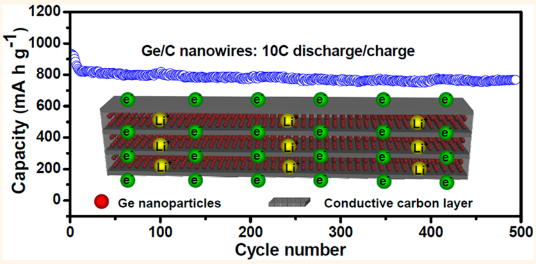

KEYWORDS: Li-ion batteries · anodes · Ge · nanowires · carbon encapsulating

The requirements to be met by lithium-ion batteries (Li-ion batteries), in terms of envisaged applications, are enormous, and the increasing demand of power density, energy density, as well as excellent cyclability has been stimulating the development of new high-performance electrode materials for Li-ion batteries.[1−3] Although the performance of Li-ion batteries continues to improve, their energy density, cycle life, and rate capability remain insufficient.[4] While replacing graphitic carbon with Si, Ge, or Sn may increase the anode capacity by about 3-fold, the rapid capacity fading during charging/discharging due to huge volume change has severely hindered their applicability in practical Li-ion batteries.[5−12]

As with Si and Sn, Ge is an excellent candidate anode material for Li-ion batteries[5−10] due to its high theoretical capacity (1600 mA h g^{-1}, 4.4 Li atoms per Ge atom theoretically, while 3.75 Li atoms are usually observed at room temperature) delivered by the alloying process, substantial lithium diffusivity (400 times faster than in Si), and high electrical conductivity (104 times higher than Si).[11,12] However, similar to Si and Sn, Ge also suffers from large volume changes during Li alloying/dealloying reactions on prolonged cycling.[13] The increasing mechanical stress causes electrode pulverization, which leads to fast capacity fading.[14] To buffer such huge volume changes during Li alloying/dealloying reactions, strategies for nanostructures of different dimensionalities such as nanoparticles, nanowires, nanotubes, as well as for nanoporous structures have been reported.[15−23] Among these morphologies, nanowires or nanotubes are considered to be most attractive due to sufficient electronic conduction of the individual wires or tubes, short Li-ion diffusion distance, and high interfacial contact area with organic electrolytes as well as easy

* Address correspondence to yanyumse@ustc.edu.cn.

Received for review April 8, 2014 and accepted June 18, 2014.

10.1021/nn501945f

percolation of the nanowires (nanotubes) network.[11,14,16,21] Recently, Ge nanowires,[11] carbon-coated Ge nanowires,[14] and graphene-coated Ge nanowires[21] have been reported as anode materials for Li-ion batteries, featuring high performances. For instance, Cui *et al.* reported that the possibility of vapor−liquid−solid (VLS) growth using direct chemical vapor deposition from GeH_4 decomposition on current collectors covered with Au catalyst could lead to Ge nanowires with Au catalyst nanoparticles. The authors demonstrated a high stable discharge capacity of 1141 mA h g^{-1} over 20 cycles at a 0.05C rate.[11] Cho *et al.* presented a similar solid−liquid−solid (SLS) growth using Bi catalyst nanoparticles for Ge nanowires coated with thin carbon layers, exhibiting a reversible charge capacity of 963 mA h g^{-1} at 0.5C.[14] However, all these reported Ge nanowire-based anode materials are synthesized with very expensive chemicals such as GeH_4 or $GeCl_4$,[5,11,21] and the finally achieved Ge nanowires contain unavoidable metal catalyst nanoparticles (*e.g.*, Au and Bi),[14,17] which will reduce the Li storage performance of Ge nanowires. Furthermore, such carbon postcoated methods (*e.g.*, C_2H_2 or CH_4 decomposition on the surface of Ge nanowires) yielded Ge nanowires with only surface-coated carbon materials, while the inner Ge nanowire matrix failed to contact with exterior conductive carbon materials.

Herein, we synthesize fully and homogeneously carbon-encapsulated Ge and GeO_x nanowires by a one-step controlled pyrolysis of organic−inorganic hybrid GeO_x/ethylenediamine (GeO_x/EDA) nanowires with self-assembled alternating GeO_x and EDA layers in H_2/Ar and Ar atmospheres, respectively. Two different self-assembled Ge-based anode materials could be obtained, namely, Ge/C nanowires (carbon-encapsulated Ge nanowires) and GeO_x/C nanowires (carbon-encapsulated GeO_x nanowires). Both types displayed excellent cycling stability at 0.2C for over 50 cycles, and Ge/C nanowires also exhibited stable and high capacities at 20C for over 200 cycles.

RESULTS AND DISCUSSION

The organic−inorganic hybrid GeO_x/EDA precursor nanowires with a sub-nanometer periodic structure are synthesized in high yield *via* a facile low-temperature solvothermal method with less expensive GeO_2 as reactant. The synthesis of GeO_x/EDA nanowires was carried out by mixing GeO_2 with Fe_2O_3 and then solvothermally treating the mixture in an aqueous EDA solution at 200 °C for 72 h. The anisotropic growth of 1D organic−inorganic hybrid GeO_x/EDA nanowires was ascribed to an Fe_2O_3-assisted self-assembly mechanism, in which the H-bonding of (N−H···O−Ge) generated by the direct assistance of Fe_2O_3 induces anisotropic growth of these hybrid nanowires,[24] similar to the solvent coordination molecular template mechanism for the growth of 1D metal chalcogenides and $Mg(OH)_2$.[25−28] In these organic−inorganic hybrid nanowires, organic EDA molecules intercalate into the inorganic GeO_x framework to form hybrid nanowires with a sub-nanometer-scale period. The inorganic units are connected by EDA *via* H-bonding of (N−H···O−Ge) (Scheme 1). Following a facile pyrolysis of these organic−inorganic hybrid GeO_x/EDA nanowires in mixed H_2/Ar or pure Ar atmospheres, fully and homogeneously carbon-encapsulated Ge or GeO_x nanowires were finally achieved (Scheme 1). Unlike the previous reported synthesis of Ge nanowire-based anode materials for Li-ion batteries, this procedure is much more convenient and has the potential of large-scale manufacturing.

Figure 1a shows a typical scanning electron microscopy (SEM) image of organic−inorganic hybrid GeO_x/EDA precursor-based nanowires, displaying that the as-obtained precursors possess a uniform, wirelike morphology with a diameter of 50−100 nm and a length of several tens of micrometers (Figure S1, Supporting Information). High-magnification SEM image (inset of Figure 1a) exhibits the rectangular section shape of these GeO_x/ethylenediamine nanowire precursors. Correspondingly, the X-ray diffraction (XRD) pattern displays an intensive diffraction peak at $2\theta = 7.93°$ (*i.e.*, $d = 1.113$ nm, Figure 1b). All diffraction peaks in Figure 1b are in good agreement with a previous report on monoclinic GeO_x/EDA products.[24] SEM images and XRD patterns of the samples annealed at different atmospheres are shown in Figure 1c−f. After annealing, both GeO_x/C (Figure 1c) and Ge/C (Figure 1e) nanowires were found to remain invariant, and also the diameter of these nanowire products displays only unremarkable changes. When the nanowire precursors were annealed in pure Ar atmospheres, the as-prepared GeO_x/C products showed amorphous structure (Figure 1d), and the conductive carbon component in GeO_x/C nanowires was converted from pyrolysis of organic EDA in precursor nanowires. All the diffraction peaks of Ge/C products (Figure 1f) calcined in H_2/Ar atmosphere can be indexed to the diamond cubic phase (JCPDS No. 04-0545).

Transmission electron microscopy (TEM) investigations of these nanowire precursors and products are shown in Figure 2. The low-magnification TEM image displayed in Figure 2a shows that organic−inorganic hybrid GeO_x/EDA precursors are single-crystalline 1D belt-like nanowires (the inset of Figure 2a). The high-magnification TEM image in Figure 2b exhibits a clear visible set of periodic black/white fringes, with a period of approximately 1.10 nm, which is consistent with the XRD results. The GeO_x/EDA nanowires provide a facile approach to achieve GeO_x/C and Ge/C nanowires for their unique sub-nanometer contact, resulting in an organic−inorganic hybrid structure. The TEM images in Figure 2c,e show that they are kept isolated without agglomeration. However, the periodic structure in

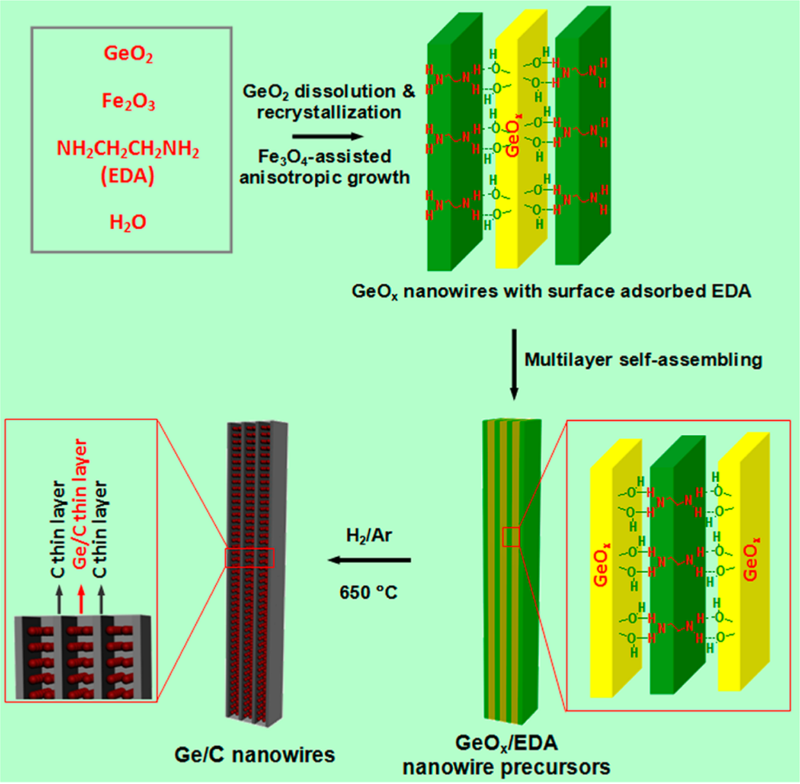

Scheme 1. Schematic representation of the fabrication of ultra-uniform carbon-encapsulated Ge/C composite nanowires from organic−inorganic hybrid GeO$_x$/EDA nanowires with self-assembled alternating GeO$_x$ and EDA layers.

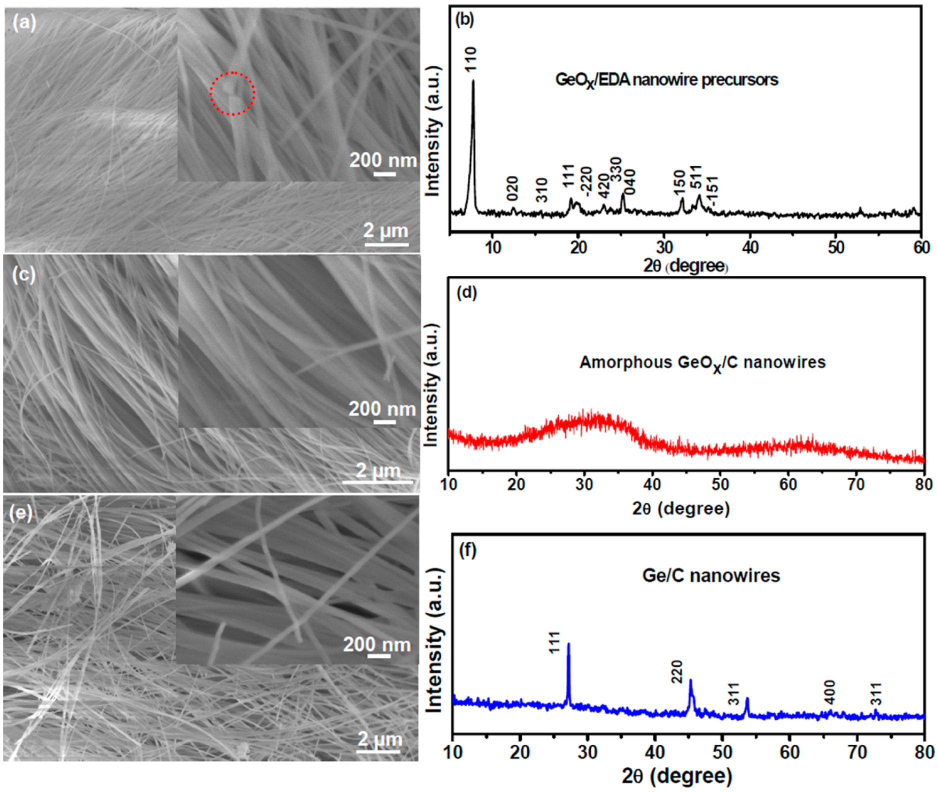

Figure 1. SEM images (a,c,e) of different magnifications and XRD patterns (b,d,f) of GeO$_x$/EDA nanowire precursors (a,b), GeO$_x$/C (c,d), and Ge/C (e,f) nanowires products. The red circle in the inset of (a) shows the rectangular section shape of GeO$_x$/EDA nanowire precursors.

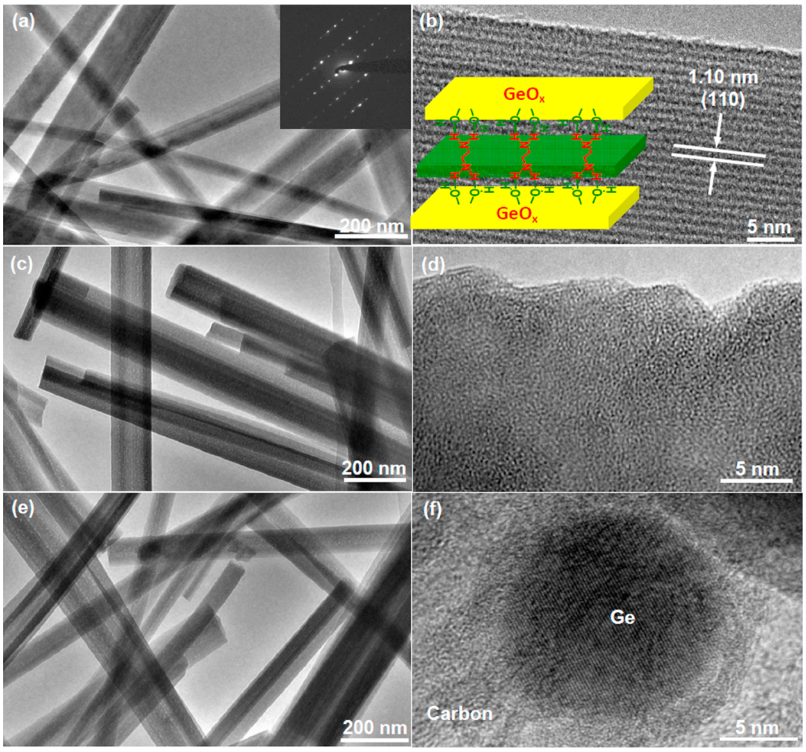

Figure 2. TEM images of of GeO_x/EDA nanowire precursors (a,b), GeO_x/C (c,d), and Ge/C (e,f) nanowires products: (a,c,e) low-magnification TEM images of GeO_x/EDA nanowire precursors (a), GeO_x/C (c), and Ge/C (e) nanowires products; (b,d,e) high-magnification TEM images of the corresponding GeO_x/EDA nanowire precursors (b), GeO_x/C (d), and Ge/C (f) nanowires products, which clearly show the multilayer structured of single-crystalline GeO_x/EDA nanowire precursors (SAED pattern shown in the inset of (a)), amorphous GeO_x/C, and well-crystallized Ge/C products.

GeO_x/EDA nanowire precursors disappears after calcination, as shown in the high-resolution TEM (HRTEM) images (Figure 2d,f). Instead, an amorphous structure in the case of GeO_x and a crystalline structure in the case of Ge emerge as displayed by these HRTEM images. Compared with GeO_x/C nanowires, Ge/C nanowires exhibit rougher and more nanoporous surfaces, which may be ascribed to further volume loss by reduction of GeO_x into Ge by H_2 during calcination.[29] The carbon content in the final Ge/C nanowires is determined as approximately 4.3% by thermogravimetric analysis (TGA, Figure S2 in Supporting Information). Figure S3 (in Supporting Information) shows the isothermal curves of both GeO_x/C and Ge/C samples from Brunauer–Emmett–Teller (BET) analysis, from where the total surface areas could be determined to be 33 and 223 m^2g^{-1}, respectively, for GeO_x/C and Ge/C nanowires.

The Ge/C nanowires with large exposed surface (S_{BET} = 223 m^2 g^{-1}) and homogeneously carbon-encapsulated characteristics are expected to show high specific capacities and excellent rate capabilities as anode materials in Li-ion batteries. This is indeed confirmed by the experiment. Figure 3a shows a typical voltage profile *versus* lithium at a cycling rate of 0.2C (320 mA g^{-1}) between 0.01 and 1.5 V. The discharge and charge capacities of the first cycle were 1748 and 1428 mA h g^{-1} (the specific capacity calculated in this paper is based on the mass of pure Ge), respectively, corresponding to a Coulombic efficiency of 82%. Compared to previous reports on Ge nanowires (prepared by a direct VLS growth using GeH_4), Ge/C nanowires (synthesis by a SLS growth using $GeCl_4$), and Ge nanotubes (prepared form Ge nanowires by a SLS growth using $GeCl_4$),[11,14,21] our Ge/C nanowires show improved capacities and efficiencies. Figure 3b displays the cycling performance and Coulombic efficiency of a Ge/C anode at 0.2C rate for 50 cycles in the voltage range of 0.01 to 1.5 V. After 50 cycles, it can still deliver a reversible capacity of 1200 mA h g^{-1}, reaching 84% of the first charge capacity, whereas the Coulombic efficiency stays higher than 90% after two cycles. Discharge/charge curves at different current densities show that these Ge/C nanohybrid materials exhibit a fairly good rate capability as anode materials (Figure 3c). Even at high current density as high as 20C, this material can still deliver a reversible discharge capacity of 690 mA h g^{-1}. Figure 3d demonstrates the remarkable rate capability of Ge/C nanowire anode, with the charge capacity of 1240, 877, and 792 mA h g^{-1} at 2C, 5C, and 10C, respectively. As shown in Figure 3d, these nanohybrid anode materials display a high steady value of 877 and 792 mA h g^{-1} at high rates of 5C and 10C, respectively.

Compared to elemental Ge, the less expensive germanium oxides could also be considered as anode materials for Li-ion batteries,[30–32] as germanium

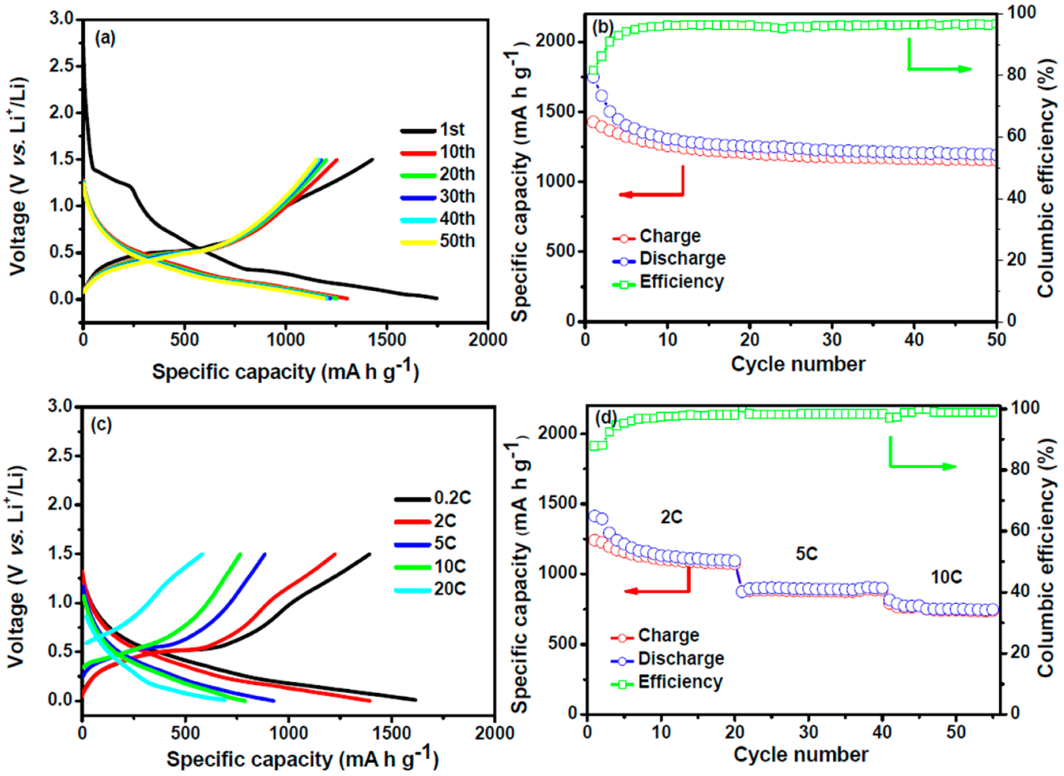

Figure 3. Electrochemical performances of Ge/C composite nanowires with fully and homogeneously carbon encapsulation: (a) voltage profiles of Ge/C composite nanowires after 1, 10, 20, 30, 40, and 50 cycles between 0.01 and 1.5 V at a charge/discharge rate of 0.2C; (b) plot of specific capacity and Coulombic efficiency of (a) as a function of cycle number; (c) voltage profiles of Ge/C composite nanowires at different rates (increased from 0.2C to 20C) between 0.01 and 1.5 V, charge and discharge rates were the same; (d) plot of specific capacity *versus* cycle number at different rates.

oxides are irreversibly reduced by Li to form Li_2O ($GeO_x + 2x\mathrm{Li} \rightarrow \mathrm{Ge} + x\mathrm{Li}_2\mathrm{O}$) and elemental Ge which further reversibly alloys with Li ($\mathrm{Ge} + 4.4\mathrm{Li} \leftrightarrow \mathrm{Li}_{4.4}\mathrm{Ge}$ theoretically, while 3.75 Li atoms are usually observed at room temperature).[31] Based on these two reactions, GeO and GeO_2 have a theoretical reversible capacity of 1356 and 1100 mA h g^{-1}, respectively. Previous research on germanium oxide anode materials suggested that cycling stability could be improved by engineering size and morphology.[30,32] The cyclic voltammetry curves (Figure S4 in Supporting Information) of ultra-uniform Ge/C and GeO_x/C nanowires have good reversibility and relatively fast kinetics. The detailed Li-ion storage performances of these GeO_x/C nanowires are shown in Figure 4. Figure 4a depicts charge/discharge galvanostatic curves of the first, 10th, 20th, 30th, 40th, and 50th cycles at 0.2C, with first specific charge and discharge capacities of 1113 and 1734 mA h g^{-1}, respectively. Obviously, these unreduced GeO_x/C nanowires also show high cycling stabilities for the whole 50 cycles at 0.2C. However, compared to reduced Ge/C nanowire anodes, GeO_x/C nanowires exhibit a lower stable specific capacity of 1000 mA h g^{-1} after 50 cycles (*vs* 1200 mA h g^{-1} for Ge/C nanowires). This should be ascribed to the lower theoretical reversible capacity of germanium oxide and lower surface area of GeO_x/C nanowires. Similar to Ge/C, the rate capability at the current densities of 0.2C to 10C is similarly good (Figure 4c,d).

We also examined the cycling performance of these Ge/C and GeO_x/C nanowires at an extremely high current density of 20C during 200 cycles. Ge/C and GeO_x/C nanowires have similar morphology and size, but oxidation affects the electrochemical performance of Ge alloy electrodes as oxygen reacts with lithium, affecting Coulombic efficiency and cycle performance.[16] For Ge/C nanowires, the cycling performance is excellent with a high stable discharge capacity of about 400 mA h g^{-1} after 200 cycles (Figure 5a), and the TEM image (Figure S5 in Supporting Information) confirms their intact nanowire morphology even after such long cycles. In terms of reversible capacities, the GeO_x/C nanowires show lower capacity of 337 mA h g^{-1} after 200 cycles at 20C (Figure 5b). As far as cycling behavior is concerned, we also examined the cycling performance of these Ge/C nanowires at a high current density of 10C for as many as 500 cycles. Over the whole period, marvelous cycling performance is exhibited, producing high stable discharge capacities of about 770 mA h g^{-1} after 500 cycles at 10C (Figure 5c). The rate capability of these uniform carbon-coated Ge/C nanowires is superior to various Ge-based high rate electrodes reported recently (Figure 5d), including pure Ge nanowire,[11]

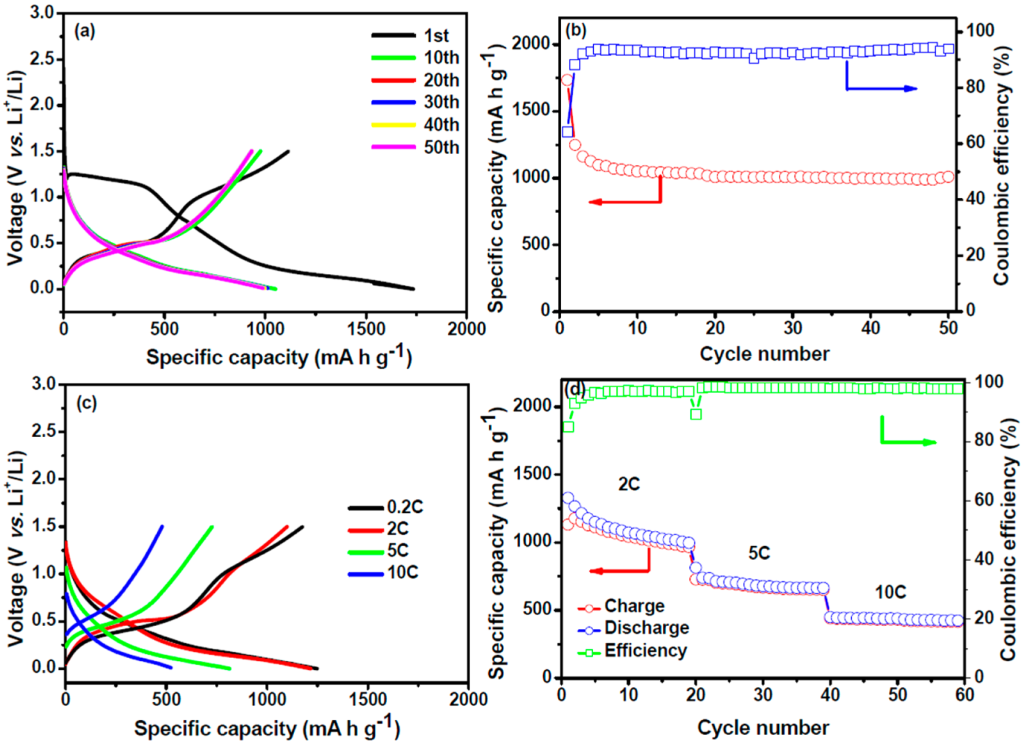

Figure 4. Electrochemical performances of ultra-uniform GeO_x/C composite nanowires: (a) voltage profiles of GeO_x/C composite nanowires after 1, 10, 20, 30, 40, and 50 cycles between 0.01 and 1.5 V at a charge/discharge rate of 0.2C; (b) plot of specific capacity and Coulombic efficiency of (a) as a function of cycle number; (c) voltage profiles of GeO_x/C composite nanowires at different rates (increased from 0.2C to 10C) between 0.01 and 1.5 V, charge and discharge rates were the same; (d) plot of specific capacity *versus* cycle number at different rates.

Ge/C nanoparticles,[12] Ge/C nanowires,[14] Ge nanotubes,[16] Ge/graphene particles,[18] Ge/graphene nanowires,[21] and Ge/Au porous composites.[23] The long cycle life with high capacity retention realized in the Ge/C nanowires seems to be attributable to complete and homogeneous carbon encapsulation of the entire Ge nanowire along both the longitudinal and lateral directions of 1D nanowires to release the mechanical strain effectively.[21] The mechanical strain of the Ge nanowires during charge/discharge processes is effectively suppressed by the exterior and interior carbon layers in the Ge/C nanowires derived from organic–inorganic hybrid GeO_x/EDA.[33−36] Moreover, homogeneously encapsulated carbon converted from the pyrolysis of organic EDA is beneficial for the overall electron communication during the cycles (Figure 5e). As discussed in the previous research,[37−41] the nanoporous carbons prepared from the pyrolysis of polymer and carbohydrates (in the current work, derived from organic EDA) will form interconnected nanochannels and electronically conductive walls, which are characteristically good conducting networks for both Li^+ and e^-.[41,42]

CONCLUSION

In conclusion, a controlled pyrolysis and reduction strategy is described to prepare Ge/C and GeO_x/C nanowires based on organic–inorganic hybrid GeO_x/EDA nanowires. During calcination in inert and reductive atmospheres, the organic–inorganic hybrid precursors undergo carbonization and reduction reactions, leading to homogeneously carbon-encapsulated structures maintaining the original morphology. The as-obtained Ge/C and GeO_x/C nanowires possess well-defined 0D-in-1D morphology and homogeneous carbon encapsulation, which exhibit excellent Li storage properties including high specific capacities (approximate 1200 and 1000 mA h g^{-1} at 0.2C for Ge/C and GeO_x/C, respectively). The Ge/C nanowires, in particular, demonstrate superior rate capability with excellent capacity retention and stability (producing high stable discharge capacities of about 770 mA h g^{-1} after 500 cycles at 10C), making them promising candidates for future electrodes for high-power Li-ion batteries.

METHODS

Ge/C and GeO_x/C Nanowires Synthesis. Organic–inorganic hybrid GeO_x/EDA nanowire precursors were synthesized by a facile and low-cost solvothermal route. In a typical procedure, 4 g of GeO_2 and 1 g of Fe_2O_3 were transferred to a 200 mL Teflon-lined stainless-steel autoclave filled with 32 mL of H_2O and 20 mL of EDA. After solvothermal treatment at 200 °C for 72 h, the top floated products were collected, then thoroughly washed with

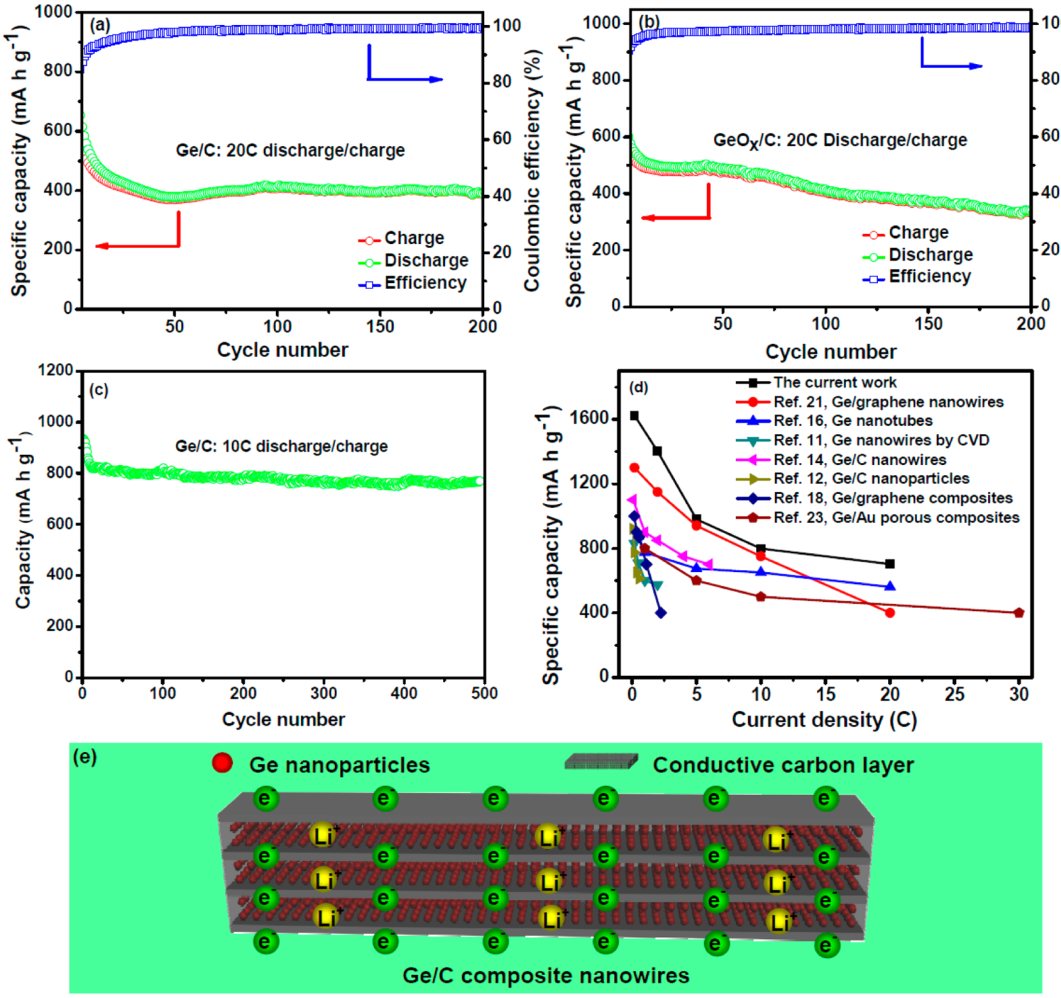

Figure 5. (a,b) Capacity and Coulombic efficiency of Ge/C and GeO$_x$/C composite nanowires continually cycled at a constant current rate of 20C over 200 cycles; (c) charge−discharge capacities of Ge/C composite nanowires over 500 cycles at 10C; (d) comparison of rate capability of various Ge-based high rate electrodes reported recently; (e) schematic representation of the electrochemical reaction path of Ge/C self-assembled composite nanowires.

ethanol and distilled water three times, and finally dried at 60 °C under vacuum. The fully and homogeneously carbon-encapsulated Ge/C and GeO$_x$/C nanowire products were finally obtained *via* calcination of these organic−inorganic hybrid GeO$_x$/EDA nanowire precursors at 650 °C for 6 h under H_2 (5%)/Ar and pure Ar atmospheres, respectively. The heating rate used throughout the experiment was 5 °C per minute, and the gas was introduced at a flow rate of 90 sccm. The yield of the Ge/C nanowires obtained *via* the current method is very high, about 95%.

Material Characterization. The collected products were characterized by X-ray diffractometry on a Rigaku-DMax 2400 diffractometer equipped with the graphite monochromatized Cu Kα radiation flux at a scanning rate of 0.02° s^{-1}. Scanning electron microscopy analysis was carried out using a Zeiss Gemini DSM 982 scanning electron microscope. The thermogravimetric analysis (TGA) was performed from room temperature to 900 °C at a ramp rate of 20 °C/min with an air flow rate of 20 mL/min using Q50 TGA. The structures of the GeO$_x$/EDA, Ge/C, and GeO$_x$/C nanowires were investigated by means of transmission electron microscopy (Zeiss EM912 Omega).

Electrochemical Test. The electrochemical performances of the as-prepared products were measured by using two-electrode Swagelok-type cells. For the preparation of the working electrode, a mixture of Ge/C or GeO$_x$/C nanowires, carbon black, and polyvinylidene fluoride in the weight ratio of 85:5:10 was ground in a mortar with *N*-methy1,2-pyrrolidone as solvent to make a slurry. For assembling Li-ion batteries, a Li foil was used as the counter electrode and a solution of 1 M $LiPF_6$ in ethylene carbonate/diethyl carbonate (1:1 in volume) was used as electrolyte. The charge/discharge curves and cycling capacity were evaluated by an Arbin MSTAT battery test system in the cutoff voltages of 0.01 and 1.5 V. Cyclic voltammetry was performed using a VoltaLab 80 electrochemical workstation.

Conflict of Interest: The authors declare no competing financial interest.

Acknowledgment. This work was financially supported by the Sofja Kovalevskaja award of the Alexander von Humboldt Foundation, the National Natural Science Foundation of China (Nos. 21171015 and 21373195), the Recruitment Program of Global Experts, program for New Century Excellent Talents in University (NCET), the Fundamental Research Funds for the Central Universities (WK2060140014, WK2060140016), and Max Planck Society. K.S. acknowledges financial support from the Doctor Training Program between the Max Planck Society and the Chinese Academy Science. The research leading to these results has received funding from the European Union Seventh Framework Programme (FP7/2007-2013) under Grant Agreement No. 312483 (ESTEEM2).

Supporting Information Available: Additional information and figures. This material is available free of charge *via* the Internet at http://pubs.acs.org.

REFERENCES AND NOTES

1. Tarascon, J. M.; Armand, M. Issues and Challenges Facing Rechargeable Lithium Batteries. *Nature* **2001**, *414*, 359–367.
2. Nam, K. T.; Kim, D. W.; Yoo, P. J.; Chiang, C. Y.; Meethong, N.; Hammond, P. T.; Chiang, M.; Belcher, A. M. Virus-Enabled Synthesis and Assembly of Nanowires for Lithium Ion Battery Electrodes. *Science* **2006**, *312*, 885–888.
3. Maier, J. Thermodynamics of Electrochemical Lithium Storage. *Angew. Chem., Int. Ed.* **2013**, *52*, 4998–5026.
4. Choi, N. S.; Chen, Z.; Freunberger, S. A.; Ji, X.; Sun, Y. K.; Amine, K.; Yushin, G.; Nazar, L. F.; Cho, J.; Bruce, P. G. Challenges Facing Lithium Batteries and Electrical Double-Layer Capacitors. *Angew. Chem., Int. Ed.* **2012**, *51*, 9994–10024.
5. Chan, C. K.; Peng, H. L.; Liu, G.; Mcilwrath, K.; Zhang, X. F.; Huggins, R. A.; Cui, Y. High-Performance Lithium Battery Anodes Using Silicon Nanowires. *Nat. Nanotechnol.* **2008**, *3*, 31–35.
6. Magasinski, A.; Dixon, P.; Hertzberg, B.; Kvit, A.; Ayala, J.; Yushin, G. High-Performance Lithium-Ion Anodes Using a Hierarchical Bottom-Up Approach. *Nat. Mater.* **2010**, *9*, 353–358.
7. Yu, Y.; Gu, L.; Zhu, C.; Tsukimoto, S.; van Aken, P. A.; Maier, J. Reversible Storage of Lithium in Silver-Coated Three-Dimensional Macroporous Silicon. *Adv. Mater.* **2010**, *22*, 2247–2250.
8. Yu, Y.; Gu, L.; Zhu, C.; van Aken, P. A.; Maier, J. Tin Nanoparticles Encapsulated in Porous Multichannel Carbon Microtubes: Preparation by Single-Nozzle Electrospinning and Application as Anode Material for High-Performance Li-Based Batteries. *J. Am. Chem. Soc.* **2009**, *131*, 15984–15985.
9. Yu, Y.; Gu, L.; Wang, C.; Dhanabalan, A.; van Aken, P. A.; Maier, J. Encapsulation of Sn@Carbon Nanoparticles in Bamboo-like Hollow Carbon Nanofibers as an Anode Material in Lithium-Based Batteries. *Angew. Chem., Int. Ed.* **2009**, *48*, 6485–6489.
10. Yu, Y.; Gu, L.; Lang, X.; Zhu, C.; Fujita, T.; Chen, M. W.; Maier, J. Li Storage in 3D Nanoporous Au-Supported Nanocrystalline Tin. *Adv. Mater.* **2011**, *23*, 2443–2447.
11. Chan, C. K.; Zhang, X. F.; Cui, Y. High Capacity Li Ion Battery Anodes Using Ge Nanowires. *Nano Lett.* **2008**, *8*, 307–309.
12. Cui, G.; Gu, L.; Zhi, L.; Kaskhedikar, N.; van Aken, P. A.; Mullen, K.; Maier, J. A Germanium−Carbon Nanocomposite Material for Lithium Batteries. *Adv. Mater.* **2008**, *20*, 3079–3083.
13. Cui, G.; Gu, L.; Kaskhedikar, N.; van Aken, P. A.; Maier, J. A Novel Germanium/Carbon Nanotubes Nanocomposite for Lithium Storage Material. *Electrochim. Acta* **2010**, *55*, 985–988.
14. Seo, M.; Park, M.; Lee, K. T.; Kim, K.; Kim, J.; Cho, J. High Performance Ge Nanowire Anode Sheathed with Carbon for Lithium Rechargeable Batteries. *Energy Environ. Sci.* **2011**, *4*, 425–428.
15. Park, M.; Kim, K.; Kim, J.; Cho, J. Flexible Dimensional Control of High-Capacity Li-Ion-Battery Anodes: From 0D Hollow to 3D Porous Germanium Nanoparticle Assemblies. *Adv. Mater.* **2010**, *22*, 415–418.
16. Park, M.; Cho, Y.; Kim, K.; Kim, J.; Liu, M.; Cho, J. Germanium Nanotubes Prepared by Using the Kirkendall Effect as Anodes for High-Rate Lithium Batteries. *Angew. Chem., Int. Ed.* **2011**, *50*, 9647–9650.
17. Gu, J.; Collins, S. M.; Carim, A. I.; Hao, X.; Bartlett, B. M.; Maldonado, S. Template-Free Preparation of Crystalline Ge Nanowire Film Electrodes *via* an Electrochemical Liquid−Liquid−Solid Process in Water at Ambient Pressure and Temperature for Energy Storage. *Nano Lett.* **2012**, *12*, 4617–4623.
18. Xue, D.; Xin, S.; Yan, Y.; Jiang, K.; Yin, Y.; Guo, Y.; Wan, L. Improving the Electrode Performance of Ge through Ge@C Core−Shell Nanoparticles and Graphene Network. *J. Am. Chem. Soc.* **2012**, *134*, 2512–2515.
19. Seng, K. H.; Park, M.; Guo, Z. P.; Liu, H. K.; Cho, J. Self-Assembled Germanium/Carbon Nanostructures as High-Power Anode Material for the Lithium-Ion Battery. *Angew. Chem., Int. Ed.* **2012**, *51*, 5657–5661.
20. Hau, K.; Park, M.; Guo, Z. P.; Liu, H. K.; Cho, J. Catalytic Role of Ge in Highly Reversible GeO$_2$/Ge/C Nanocomposite Anode Material for Lithium Batteries. *Nano Lett.* **2013**, *13*, 1230–1236.
21. Kim, H.; Son, Y.; Park, C.; Cho, J.; Choi, H. C. Catalyst-Free Direct Growth of a Single to a Few Layers of Graphene on a Germanium Nanowire for the Anode Material of a Lithium Battery. *Angew. Chem., Int. Ed.* **2013**, *52*, 5997–6001.
22. Yan, C.; Xi, W.; Si, W.; Deng, J.; Schmidt, O. G. Highly Conductive and Strain-Released Hybrid Multilayer Ge/Ti Nanomembranes with Enhanced Lithium-Ion-Storage Capability. *Adv. Mater.* **2013**, *25*, 539–544.
23. Yu, Y.; Yan, C.; Gu, L.; Lang, X.; Tang, K.; Zhang, L.; Hou, Y.; Wang, Z.; Chen, M. W.; Schmidt, O. G.; *et al.* Three-Dimensional (3D) Bicontinuous Au/Amorphous-Ge Thin Films as Fast and High-Capacity Anodes for Lithium-Ion Batteries. *Adv. Energy Mater.* **2013**, *3*, 281–285.
24. Gao, Q.; Chen, P.; Zhang, Y.; Tang, Y. Synthesis and Characterization of Organic−Inorganic Hybrid GeOx/Ethylenediamine Nanowires. *Adv. Mater.* **2008**, *20*, 1837–1842.
25. Li, Y. D.; Liao, H. W.; Ding, Y.; Fan, Y.; Zhang, Y.; Qian, Y. T. Solvothermal Elemental Direct Reaction to CdE (E = S, Se, Te) Semiconductor Nanorod. *Inorg. Chem.* **1999**, *38*, 1382–1387.
26. Li, Y. D.; Sui, M.; Ding, Y.; Zhang, G. H.; Wang, C. Preparation of Mg(OH)$_2$ Nanorods. *Adv. Mater.* **2000**, *12*, 818–821.
27. Gao, M. R.; Yao, W. T.; Yao, H. B.; Yu, S. H. Synthesis of Unique Ultrathin Lamellar Mesostructured CoSe$_2$−Amine (Protonated) Nanobelts in a Binary Solution. *J. Am. Chem. Soc.* **2009**, *131*, 7486–7487.
28. Yao, H. B.; Gao, M. R.; Yu, S. H. Small Organic Molecule Templating Synthesis of Semiconducting Organic−Inorganic Hybrid Nanomaterials. *Nanoscale* **2010**, *2*, 323–334.
29. Liu, J.; Xue, D. Thermal Oxidation Strategy towards Porous Metal Oxide Hollow Architectures. *Adv. Mater.* **2008**, *20*, 2622–2627.
30. Pena, J. S.; Sandu, I.; Joubert, O.; Pascual, F. S.; Arean, C. O.; Brousse, T. Electrochemical Reaction between Lithium and β-Quartz GeO$_2$. *Electrochem. Solid State Lett.* **2004**, *7*, A278–A281.
31. Lin, Y. M.; Klavetter, K. C.; Heller, A.; Mullins, C. B. Storage of Lithium in Hydrothermally Synthesized GeO$_2$ Nanoparticles. *J. Phys. Chem. Lett.* **2013**, *4*, 999–1004.
32. Wang, X.; Han, W.; Chen, H.; Bai, J.; Tyson, T. A.; Yu, X.; Wang, X.; Yang, X. Amorphous Hierarchical Porous GeO$_x$ as High-Capacity Anodes for Li Ion Batteries with Very Long Cycling Life. *J. Am. Chem. Soc.* **2011**, *133*, 20692–20695.
33. Liu, J.; Liu, W.; Chen, K.; Ji, S.; Zhou, Y.; Wan, Y.; Xue, D.; Hodgson, P.; Li, Y. Facile Synthesis of Transition-Metal Oxide Nanocrystals Embedded in Hollow Carbon Microspheres for High-Rate Lithium-Ion-Battery Anodes. *Chem.—Eur. J.* **2013**, *19*, 9811–9816.
34. Liu, W.; Liu, J.; Chen, K.; Ji, S.; Wan, Y.; Zhou, Y.; Xue, D.; Hodgson, P.; Li, Y. Enhancing the Electrochemical Performance of the LiMn$_2$O$_4$ Hollow Microsphere Cathode with a LiNi$_{0.5}$Mn$_{1.5}$O$_4$ Coated Layer. *Chem.—Eur. J.* **2014**, *20*, 824–830.
35. Liu, J.; Tang, K.; Song, K.; van Aken, P. A.; Yu, Y.; Maier, J. Tiny Li$_4$Ti$_5$O$_{12}$ Nanoparticles Embedded in Carbon Nanofibers as High-Capacity and Long-Life Anode Materials for Both Li-Ion and Na-Ion Batteries. *Phys. Chem. Chem. Phys.* **2013**, *15*, 20813–20818.
36. Liu, J.; Tang, K.; Song, K.; van Aken, P. A.; Yu, Y.; Maier, J. Electrospun Na$_3$V$_2$(PO$_4$)$_3$/C Nanofibers as Stable Cathode Materials for Sodium-Ion Batteries. *Nanoscale* **2014**, *6*, 5081–5086.
37. Liu, J.; Song, K.; van Aken, P. A.; Maier, J.; Yu, Y. Self-Supported Li$_4$Ti$_5$O$_{12}$−C Nanotube Arrays as High-Rate and Long-Life Anode Materials for Flexible Li-Ion Batteries. *Nano Lett.* **2014**, *14*, 2597–2603.

38. Li, X.; Meng, X.; Liu, J.; Geng, D.; Zhang, Y.; Banis, M. N.; Li, Y.; Yang, J.; Li, R.; Sun, X.; *et al.* Tin Oxide with Controlled Morphology and Crystallinity by Atomic Layer Deposition onto Graphene Nanosheets for Enhanced Lithium Storage. *Adv. Funct. Mater.* **2012**, *22*, 1647–1654.
39. Li, X.; Dhanabalan, A.; Gu, L.; Wang, C. Three-Dimensional Porous Core−Shell Sn@Carbon Composite Anodes for High-Performance Lithium-Ion Battery Applications. *Adv. Energy Mater.* **2012**, *2*, 238–244.
40. Li, X.; Wang, C. Engineering Nanostructured Anodes via Electrostatic Spray Deposition for High Performance Lithium Ion Battery Application. *J. Mater. Chem. A* **2013**, *1*, 165–182.
41. Xin, S.; Guo, Y. G.; Wan, L. J. Nanocarbon Networks for Advanced Rechargeable Lithium Batteries. *Acc. Chem. Res.* **2012**, *45*, 1759–1769.
42. Wu, X. L.; Guo, Y. G.; Wan, L. J. Rational Design of Anode Materials Based on Group IVA Elements (Si, Ge, and Sn) for Lithium-Ion Batteries. *Chem.—Asian J.* **2013**, *8*, 1948–1958.